PHYSICAL REVIEW D **80,** 055014 (2009)

Meson wave function from holographic models

Alfredo Vega,[1] Ivan Schmidt,[1] Tanja Branz,[2] Thomas Gutsche,[2] and Valery E. Lyubovitskij[2,*]

[1]*Departamento de Física y Centro de Estudios Subatómicos, Universidad Técnica Federico Santa María, Casilla 110-V, Valparaíso, Chile*

[2]*Institut für Theoretische Physik, Universität Tübingen, Kepler Center for Astro and Particle Physics, Auf der Morgenstelle 14, D–72076 Tübingen, Germany*

(Received 5 June 2009; published 10 September 2009)

We consider the light-front wave function for the valence quark state of mesons using the AdS/CFT correspondence, as has been suggested by Brodsky and Téramond. Two kinds of wave functions, obtained in different holographic Soft-Wall models, are discussed.

DOI: 10.1103/PhysRevD.80.055014 PACS numbers: 11.25.Tq, 12.39.Ki, 14.40.Aq, 14.40.Cs

I. INTRODUCTION

The hadronic wave function in terms of quark and gluon degrees of freedoms plays an important role in QCD process predictions. For example, knowledge of the wave function allows to calculate distribution amplitudes and structure functions or conversely these processes can give phenomenological restrictions on the wave functions.

In principle the Bethe-Salpeter approach [1] and discrete quantization in the light-front formalism [2] allow to obtain hadronic wave functions but in practice several problems present to realize this [3,4]. Therefore approximate solutions for hadronic bound states are usually considered using in a first step specific quarks models to obtain the valence quark wave function.

There are several nonperturbative approaches to obtain properties of distribution amplitudes and/or hadronic wave functions from QCD, and now we have possibility to include techniques based on the anti–de Sitter space/conformal field theory (AdS/CFT) correspondence.

Although a rigorous QCD dual is unknown, a simple approach known as bottom-up allows to built models that have some essential QCD features, including counting rules at short and confinement at long distances. This model has been successful in several QCD applications such as hadronic scattering processes [5–8], hadron spectrum [9–13], hadronic couplings and chiral symmetry breaking [14–16], quark potentials [17–19] and hadron decays [20].

Together with these applications it is possible to set up a mapping between specific properties of the AdS description for hadrons and the Hamiltonian formulation for quantized QCD in the light-front formalism. This approach allows to obtain an excellent first approximation to the valence wave function for mesons [21,22]. Wave functions obtained using the AdS/CFT correspondence can be used as an initial ansatz for a variational treatment or as basis states to diagonalize the light-front QCD Hamiltonian.

In this work meson wave functions obtained in the context of AdS/CFT ideas [21,22] are studied considering two kinds of holographic soft-wall models. First we consider the more usual model with a quadratic dilaton [10,14,22]. Then we discuss predictions of a recent model which considers a logarithmic dilaton as suggested by Einstein's equations for an AdS metric. It also includes anomalous dimensions [13] and allows to reproduce the Regge behavior even in the baryonic sector.

The work is structured as follows. Sec. II is devoted to the extraction of wave functions for scalar/pseudoscalar mesons using the two holographic models. In Sec. III we concentrate on the pion wave function discussing the adjustment of the model parameters. Distribution amplitudes and parton distributions for the valence state are calculated in both models. In the pion case we consider both current and constituent quark masses. In Sec. IV we calculate decay constants in the simplified case when the valence component is dominant. Conclusions are presented in Sec. V.

II. MESON WAVE FUNCTION IN HOLOGRAPHICAL MODELS

The comparison of form factors calculated both in the light-front formalism and in AdS offers the possibility to relate AdS modes to light-front wave functions (LFWF) [21,22]. Below we briefly discuss the derivation of this matching procedure.

In the light-front formalism the electromagnetic form factor of pion can be written as [22]

$$F(Q^2) = 2\pi \int_0^1 dx \frac{1-x}{x} \int_0^\infty d\zeta \zeta J_0\left(\zeta Q \sqrt{\frac{1-x}{x}}\right) \tilde{\rho}(x,\zeta), \tag{1}$$

where $\tilde{\rho}(x,\zeta)$ is the effective transverse distribution of partons; Q^2 is the spacelike momentum transfer squared; J_0 is the Bessel function. Here we introduced the variable

*On leave of absence from Department of Physics, Tomsk State University, 634050 Tomsk, Russia.

$$\zeta = \sqrt{\frac{x}{1-x}}\left|\sum_{j=1}^{n-1} x_j \mathbf{b}_{\perp j}\right|, \tag{2}$$

which represents the x-weighted transverse impact coordinate of the spectator system.

On the other side the corresponding expression for scalars in AdS with a dilaton $\varphi(z)$ is

$$F(Q^2) = \int_0^\infty dz \Phi(z) J_\kappa(Q^2, z)\Phi(z), \tag{3}$$

where $\Phi(z)$ corresponds to modes that represent hadrons, $J(Q^2, z)$ is the dual mode to the electromagnetic current, and the metric considered is

$$\begin{aligned} ds^2 &= \frac{R^2}{z^2}\eta_{\mu\nu}dx^\mu dx^\nu, \\ \eta_{\mu\nu} &= \mathrm{diag}(1, -1, -1, -1-1), \end{aligned} \tag{4}$$

where z is the holographic coordinate and κ, that represent different things in both holographical models considered, in one model is the scale parameter characterizing the dilaton field and in the other one this characterize the anomalous dimension as you can see later when we discuss the models considered. An important step is to set up the electromagnetic current as

$$J(Q^2, z) = \int_0^1 dx g(x) J_0\left(\zeta Q\sqrt{\frac{1-x}{x}}\right). \tag{5}$$

Putting $z = \zeta$ and comparing Eqs. (1) and (3) we get

$$\tilde{\rho}(x, \zeta) = \frac{xg(x)}{1-x}\frac{|\Phi(\zeta)|^2}{2\pi\zeta}. \tag{6}$$

Finally, considering the case with two partons q_1 and $\bar{q}_2$

$$\tilde{\rho}_{n=2}(x, \zeta) = \frac{|\tilde{\psi}_{q_1\bar{q}_2}(x, \zeta)|^2}{(1-x)^2}\frac{1}{A^2}, \tag{7}$$

where $\zeta^2 = x(1-x)\mathbf{b}_\perp^2$ and A is the normalization constant, we obtain the relation between the AdS modes and the meson LFWF $\tilde{\psi}_{q_1\bar{q}_2}(x, \zeta)$

$$|\tilde{\psi}_{q_1\bar{q}_2}(x, \zeta)|^2 = A^2 x(1-x)g(x)\frac{|\Phi(\zeta)|^2}{2\pi\zeta}. \tag{8}$$

Here A is constrained by the probability condition

$$P_{q_1\bar{q}_2} = \int_0^1 dx \int d^2\mathbf{b}_\perp |\tilde{\psi}_{q_1\bar{q}_2}(x, \mathbf{b}_\perp)|^2 \leq 1 \tag{9}$$

with $P_{q_1\bar{q}_2}$ being the probability of finding the valence Fock state $|q_1\bar{q}_2\rangle$ in the meson M. Note, in the case of massless quarks we have $A = \sqrt{P_{q_1\bar{q}_2}}$, while this is not the case for massive quarks (see discussion in Sec. II A). Next we consider two kinds of holographical models (Model 1 and Model 2) and their respective wave functions.

A. Model 1

Model 1 is based on the Schrödinger equation [23]

$$\begin{aligned} &\left[-\frac{d^2}{d\zeta^2} - \frac{1-4L^2}{4\zeta^2} + \kappa_1^4\zeta^2 + 2\kappa_1^2(L+S-1)\right]\Phi_1(\zeta) \\ &= M_1^2\Phi_1(\zeta), \end{aligned} \tag{10}$$

for the AdS modes $\Phi(\zeta)$ that describe hadrons with integer spin S and the mass spectrum

$$M_1^2 = 4\kappa_1^2\left(n + L + \frac{S}{2}\right), \tag{11}$$

where n and L are the radial and orbital quantum numbers. Here subscript "1" indicates the solutions of Model 1.

In this model the function $g(x)$ in matching condition (8) is fixed as $g(x) = 1$ for large values of $Q^2 \gg 4\kappa^2$. In this case the current $J_\kappa(Q^2, z)$ decouples from the dilaton field [22]. The examples considered in this work correspond to mesons with $n = L = 0$, although both for scalars and vectors we find

$$\Phi_1(\zeta) = \kappa_1\sqrt{2\zeta}\exp^{-(1/2)\kappa_1^2\zeta^2} \sim \sqrt{\zeta}\exp^{-(1/2)\kappa_1^2\zeta^2}. \tag{12}$$

Using Eq. (12) and keeping in mind that $\zeta^2 = x(1-x)\mathbf{b}_\perp^2$, the meson LFWF of this model is

$$\tilde{\psi}^{(1)}_{q_1\bar{q}_2}(x, \mathbf{b}_\perp) = \frac{\kappa_1 A_1}{\sqrt{\pi}}\sqrt{x(1-x)}\exp\left(-\frac{1}{2}\kappa_1^2 x(1-x)\mathbf{b}_\perp^2\right). \tag{13}$$

The wave function (13) does not consider massive quarks. We include the quark masses following the prescription suggested by Brodsky and Téramond [24]. First one should perform the Fourier transform of (13)

$$\psi^{(1)}_{q_1\bar{q}_2}(x, \mathbf{k}_\perp) = \frac{4\pi A_1}{\kappa_1\sqrt{x(1-x)}}\exp\left(-\frac{\mathbf{k}_\perp^2}{2\kappa_1^2 x(1-x)}\right). \tag{14}$$

In a second step the quark masses are introduced by extending the kinetic energy of massless quarks with $K_0 = \frac{\mathbf{k}_\perp^2}{x(1-x)}$ to the case of massive quarks:

$$K_0 \to K = K_0 + \mu_{12}^2, \qquad \mu_{12}^2 = \frac{m_1^2}{x} + \frac{m_2^2}{1-x}. \tag{15}$$

Note, the change proposed in (15) is equivalent to the following change in (10)

$$-\frac{d^2}{d\zeta^2} \to -\frac{d^2}{d\zeta^2} + \mu_{12}^2. \tag{16}$$

Finally we obtain

$$\psi^{(1)}_{q_1\bar{q}_2}(x, \mathbf{k}_\perp) = \frac{4\pi A_1}{\kappa_1\sqrt{x(1-x)}}\exp\left(-\frac{\mathbf{k}_\perp^2}{2\kappa_1^2 x(1-x)} - \frac{\mu_{12}^2}{2\kappa_1^2}\right). \tag{17}$$

Note, in the case of massive quarks the normalization

constant fulfills the relation

$$A_1 = \sqrt{P_{q_1\bar{q}_2}}\left(\int_0^1 dx e^{-\mu_{12}^2/\kappa_1^2}\right)^{-1/2} \tag{18}$$

and $A_1 \to \sqrt{P_{q_1\bar{q}_2}}$ when $m_{1,2} \to 0$.

B. Model 2

Model 2 has originally been developed in Ref. [13]. It is based on the following equation of motion for the AdS modes

$$\partial_\zeta^2\varphi(\zeta) - \frac{2-\beta}{\zeta}\partial_\zeta\varphi(\zeta) + \left(M_2^2 - \frac{m_5^2R^2}{\zeta^2}\right)\varphi(\zeta) = 0, \tag{19}$$

where for mesons we have

$$m_5^2R^2 = (3 + L - S + \kappa_2^2\zeta^2)(L - S + \beta + \kappa_2^2\zeta^2). \tag{20}$$

Here subscript "2" indicates the solutions of the Model 2. From (19) we get the mass spectrum

$$M_2^2 = 4\kappa_2^2\left[n + L + \left(2 + \frac{\beta}{2} - S\right)\right], \tag{21}$$

where $\beta = -3$ is the value for scalar mesons and $\beta = -1$ for vector mesons [13]. To have consistency with the definition of the form factor of Eq. (3) the Eq. (19) should be changed into a Schrödinger type equation of

$$\left[-\frac{d^2}{d\zeta^2} + \frac{4m_5^2R^2 + \beta^2 - 6\beta + 8}{4\zeta^2}\right]\Phi_2(\zeta) = M_2^2\Phi_2(\zeta), \tag{22}$$

by means of the following transformation

$$\varphi(\zeta) = e^{(1-\beta/2)\ln\zeta}\Phi_2(\zeta). \tag{23}$$

In this model we have $g(x) = 2x$ [13] and the matching condition between the LFWF and AdS modes reads

$$|\tilde{\psi}^{(2)}_{q_1\bar{q}_2}(x,\zeta)|^2 = 2A_2^2x^2(1-x)\frac{|\Phi_2(\zeta)|^2}{2\pi\zeta}. \tag{24}$$

Again we restrict to the ground state case—$n = L = 0$ and as AdS mode $\Phi_2(\zeta)$ similar to the one of Model 1:

$$\Phi_2(\zeta) \sim \sqrt{\zeta}e^{-(1/2)\kappa_2^2\zeta^2}. \tag{25}$$

Finally applying the Brodsky and Téramond prescription, the meson momentum space LFWF including massive quarks is

$$\psi^{(2)}_{q_1\bar{q}_2}(x,\mathbf{k}_\perp) = \frac{4\pi A_2}{\kappa_2}\sqrt{\frac{2}{1-x}}\exp\left(-\frac{\mathbf{k}_\perp^2}{2\kappa_2^2x(1-x)} - \frac{\mu_{12}^2}{2\kappa_2^2}\right), \tag{26}$$

where A_2 is the normalization constant constrained by the probability condition (9) in analogy to A_1.

III. EXAMPLE I: THE PION

A. Fixing the parameters

The wave functions we consider depend on parameters $(A_i, m_{1,2}, \kappa_i)$ which must be fixed. As a first application we consider some of the fundamental properties of the pion: leptonic and two-photon decay constants, distribution quantities. We work in the isospin limit, supposing that the masses of u and d quarks are equal to each other: $m = m_u = m_d$. In this case we have a set of three free parameters (A_i, m, κ_i) which is the same number of parameters considered in other models [25].

The two conditions related to the decay amplitudes for $\pi \to \mu\nu$ and $\pi^0 \to \gamma\gamma$ [26] read

$$\int_0^1 dx \int \frac{d^2\mathbf{k}_\perp}{16\pi^3}\psi_{q\bar{q}}(x,\mathbf{k}_\perp) = \frac{F_\pi}{2\sqrt{3}}, \tag{27}$$

and

$$\int_0^1 dx\psi_{q\bar{q}}(x,\mathbf{k}_\perp = 0) = \frac{\sqrt{3}}{F_\pi}, \tag{28}$$

where $F_\pi = f_\pi/\sqrt{2} \simeq 92.4$ MeV is the pion leptonic decay constant. Note, the second condition (28) is the low-energy theorem relating the two-photon $g_{\pi\gamma\gamma}$ and leptonic F_π decay constants as $g_{\pi\gamma\gamma} = 1/(4\pi^2F_\pi) = 0.274\ \text{GeV}^{-1}$.

On the other side, the average transverse momentum squared of a quark in the pion $\langle\mathbf{k}_\perp^2\rangle_\pi$ is about $(300\ \text{MeV})^2$ [27]. The average transverse momentum squared of a quark in the pion valence state is defined by

$$\langle\mathbf{k}_\perp^2\rangle_{q\bar{q}} = \frac{1}{P_{q\bar{q}}}\int_0^1 dx\int\frac{d^2\mathbf{k}_\perp}{16\pi^3}\mathbf{k}_\perp^2|\psi_{q\bar{q}}(x,\mathbf{k}_\perp)|^2, \tag{29}$$

which must be higher than $\langle\mathbf{k}_\perp^2\rangle_\pi$. For this reason we consider a value of several hundreds of MeV for $\sqrt{\langle\mathbf{k}_\perp^2\rangle_{q\bar{q}}}$. This can be used as a third restriction. When fixing the parameters we consider two cases for each wave function (17) and (26), current and constituent quark masses. The values used are 4 MeV for current masses and 330 MeV for constituent masses.

Since quarks masses are introduced in advance, the remaining parameters A_i and κ_1 or κ_2 can be fixed using (27) and (28) with the value of $F_\pi = 92.4$ MeV. Then with

TABLE I. Parameters defining LFWF given by Eqs. (17) and (26) and predictions for $\sqrt{\langle\mathbf{k}_\perp^2\rangle_{q\bar{q}}}$ and $P_{q\bar{q}}$.

Model	$\psi(x,\mathbf{k}_\perp)$	m (MeV)	A	κ (MeV)	$\sqrt{\langle\mathbf{k}_\perp^2\rangle_{q\bar{q}}}$ (MeV)	$P_{q\bar{q}}$
1	ψ_{1c}	4	0.452	951.043	388.319	0.204
	ψ_{1cs}	330	0.924	787.43	356.478	0.279
2	ψ_{2c}	4	0.486	921.407	376.222	0.236
	ψ_{2cs}	330	0.965	781.218	353.877	0.299

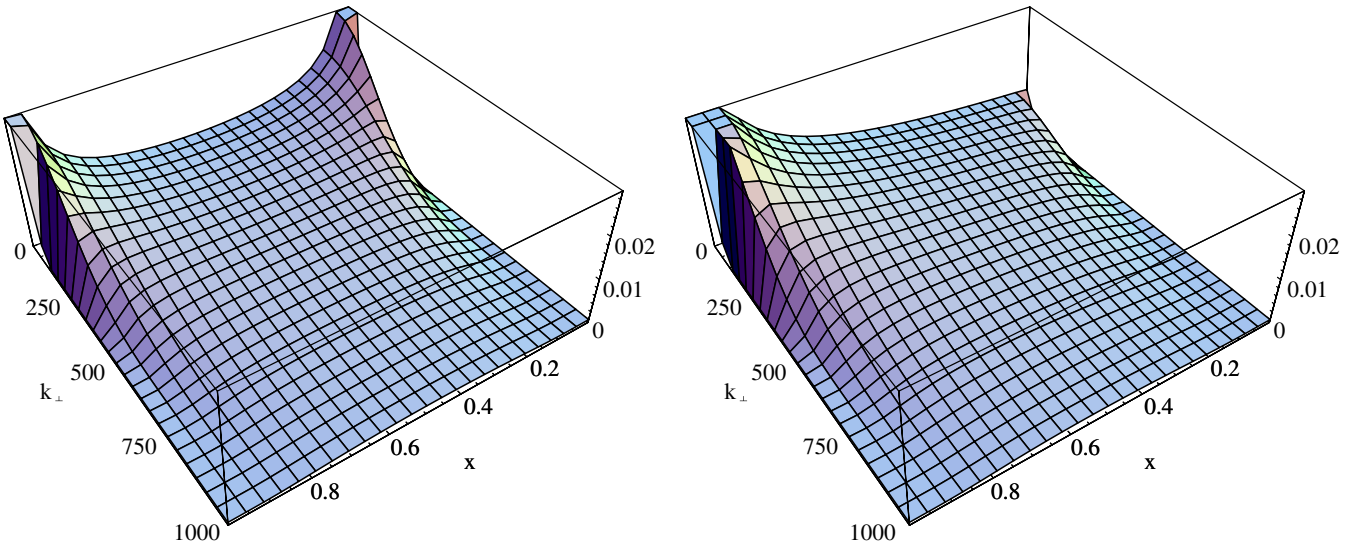

FIG. 1 (color online). The pion wave function $\psi(x, \mathbf{k}_\perp)$, for $m = 4$ MeV. The left graph corresponds to Eq. (17) and the right one to Eq. (26).

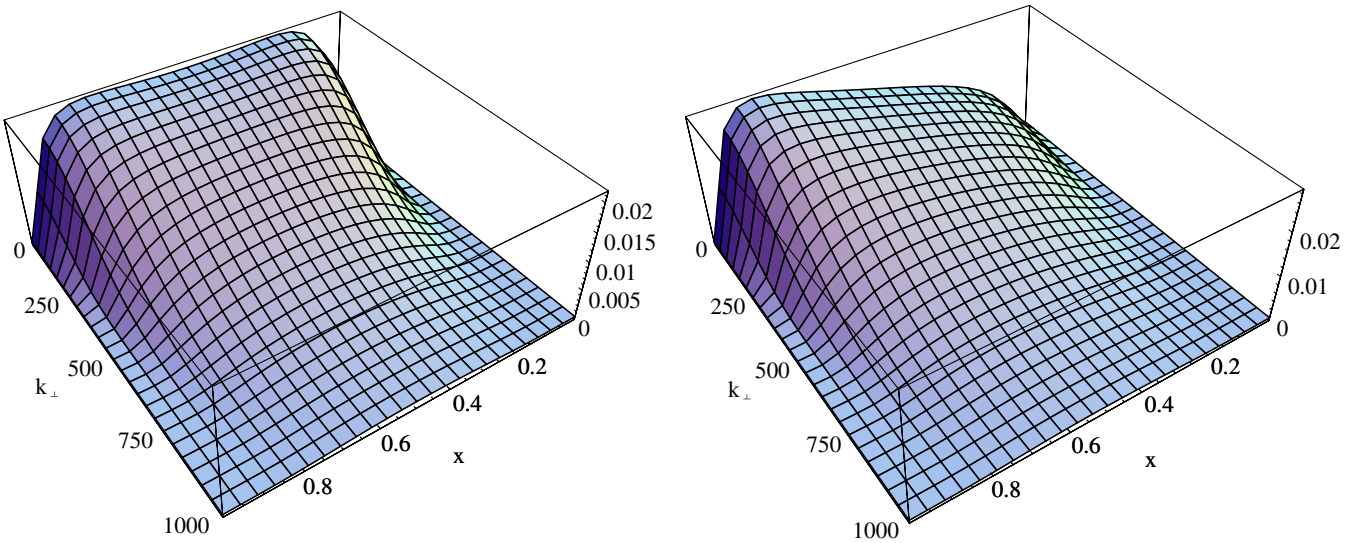

FIG. 2 (color online). The pion wave function $\psi_\pi(x, \mathbf{k}_\perp)$, for $m = 330$ MeV. The left graph corresponds to equation Eq. (17) and the right one to Eq. (26).

the fixed parameters A_i, m, κ_i we predict $\sqrt{\langle \mathbf{k}_\perp^2 \rangle_{q\bar{q}}}$ and the probability $P_{q\bar{q}}$. Table I gives the values for $A_{1,2}$ and $\kappa_{1,2}$ including the predictions for $\sqrt{\langle \mathbf{k}_\perp^2 \rangle_{q\bar{q}}}$ and $P_{q\bar{q}}$. One can see that our results for $\sqrt{\langle \mathbf{k}_\perp^2 \rangle_{q\bar{q}}}$ and $P_{q\bar{q}}$ are in agreement with the predictions of Ref. [25]: $\sqrt{\langle \mathbf{k}_\perp^2 \rangle_{q\bar{q}}} \simeq 356$ MeV and $P_{q\bar{q}} \simeq 0.296$.

The parameters $\kappa_{1,2}$ define the holographic model considered in Refs. [13,22] and both are related to the Regge slope. Thus in principle both quantities could be fixed by spectral data. Unfortunately the pion mass is an exception since it falls outside the Regge trajectories. Therefore $\kappa_{1,2}$ have been usually fixed by using form factors [13,22]. The values obtained in the present work differ somewhat from those values, which is understandable since the κ_1 and κ_2 found previously were obtained using (3), the form factor in AdS, which when compared with the light-front expression gave (6). Nevertheless, the wave functions (17) and (26) correspond to the case with only two quarks, and we therefore should expect a small change in the $\kappa_{1,2}$ values.

In Figs. 1 and 2, we consider the LFWF using parameters that appear in Table I, and additionally consider in Fig. 3 a $c\bar{c}$ case in order to show the asymmetry in x is reduced when quark mass is increased

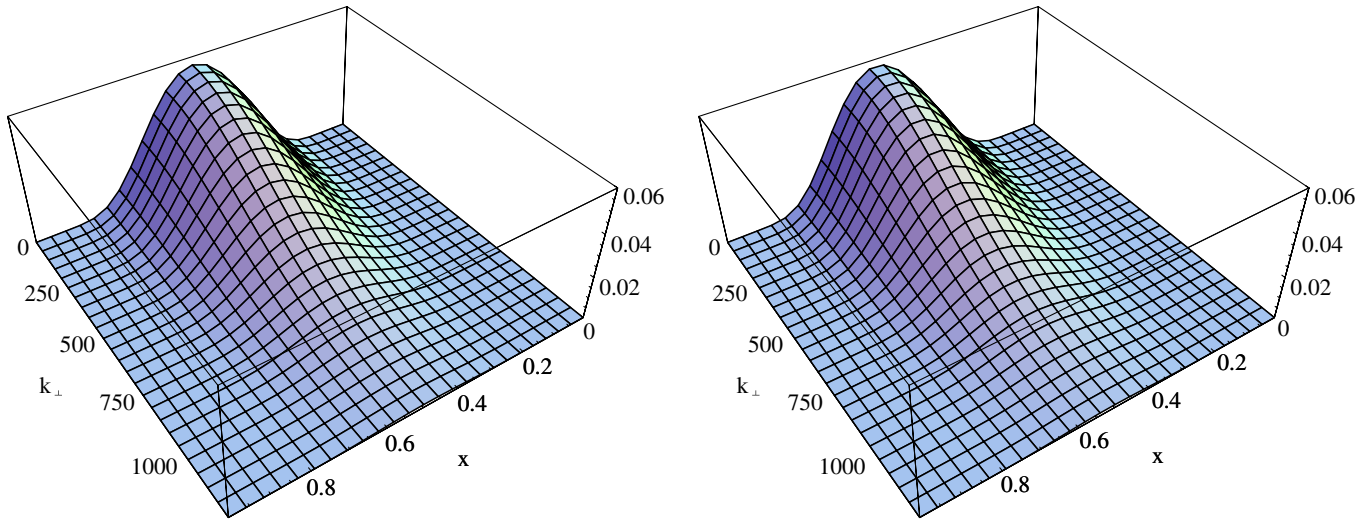

FIG. 3 (color online). Wave function $\psi_{c\bar{c}}(x, \mathbf{k}_\perp)$ according to section IV. We consider in this case $m_c = 1.5$ GeV and $\kappa_1 = \kappa_2 = 894$ MeV, the value suggested by the Regge slope for charmonium states. The left graph corresponds to Eq. (17) and the right graph to Eq. (26).

B. Pion distribution amplitude

The meson distribution amplitude is calculated using [28]

$$\phi(x, q) = \int^{q^2} \frac{d^2\mathbf{k}_\perp}{16\pi^3} \psi_{\mathrm{val}}(x, \mathbf{k}_\perp). \tag{30}$$

We remind that the pion $|\psi\rangle$ can be expanded into Fock states $|\psi\rangle = a_1|q\bar{q}\rangle + a_2|q\bar{q}g\rangle + a_3|q\bar{q}gg\rangle + \ldots$. For large values of q^2 the dominant term is the first one and since our wave functions were obtained considering (7), which corresponds to the $q\bar{q}$ configuration, we can calculate $\phi(x) \equiv \phi(x, Q \to \infty)$.

Using (17) and (26) we get

$$\phi_1(x) = \frac{A_1\kappa_1}{2\pi}\sqrt{x(1-x)}\exp\left(-\frac{m^2}{2\kappa_1^2 x(1-x)}\right), \tag{31}$$

and

$$\phi_2(x) = \frac{A_2\kappa_2}{2\pi} x\sqrt{2(1-x)}\exp\left(-\frac{m^2}{2\kappa_1^2 x(1-x)}\right). \tag{32}$$

In Fig. 4 both expressions are compared for current (c) and constituent (cs) quark masses to the prediction of PQCD using $\phi(x, Q \to \infty) = \sqrt{3}F_\pi x(1-x)$ [29]. Figure 4 shows that increasing quark masses reduces the differences between the two variants of LFWFs. Knowing the distribution amplitudes, it is possible to calculate the moments. Taking $\xi = 1 - 2x$ we have

$$\langle \xi^N \rangle = \frac{\int_{-1}^{1} d\xi \xi^N \phi(\xi)}{\int_{-1}^{1} d\xi \phi(\xi)}. \tag{33}$$

Table II contains a summary of the moments up to $\langle \xi^4 \rangle$.

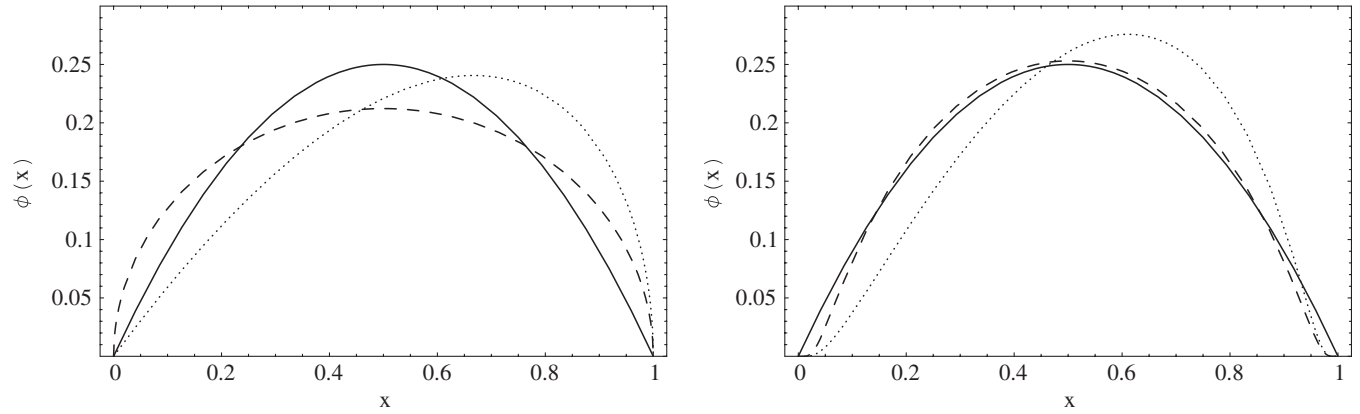

FIG. 4. Pion distribution amplitudes using holographic LFWF. Solid lines correspond to the prediction of PQCD, dashed lines correspond to LFWF (31), and the dotted ones to LFWF (32) for $m = 4$ MeV (upper panel) and for $m = 330$ MeV (lower panel).

TABLE II. First moments of the distribution functions $\langle \xi^N \rangle$ calculated using $\phi_{\rm PQCD}$ and ϕ, given explicitly by (31) and (32), for $m = 4$ MeV and $m = 330$ MeV. For ϕ_{2cs*} we take $m = 300$ MeV, which shows that odd moments are reduced when the quark mass quarks increases.

ϕ	$\langle \xi^0 \rangle$	$\langle \xi^1 \rangle$	$\langle \xi^2 \rangle$	$\langle \xi^3 \rangle$	$\langle \xi^4 \rangle$
$\phi_{\rm PQCD}$	1	0	0.2	0	0.086
ϕ_{1c}	1	0	0.250	0	0.125
ϕ_{2c}	1	0.143	0.238	0.073	0.116
ϕ_{1cs}	1	0	0.186	0	0.073
ϕ_{2cs}	1	0.102	0.179	0.040	0.068
ϕ_{2cs*}	1	0.106	0.187	0.044	0.073

C. Parton distributions

If the LFWF has the form

$$\psi_{q\bar{q}}(x, \mathbf{k}_\perp) = \eta(x) \exp\left(-\frac{\mathbf{k}_\perp^2}{2\lambda^2 x(1-x)}\right), \qquad (34)$$

then the parton distribution is given by [30]

$$f(x) = \frac{x(1-x)\lambda^2}{16\pi^2}\eta^2(x). \qquad (35)$$

The LFWFs obtained from Models 1 and 2 have the form considered in (34) and then the two-body contribution to the parton distributions can be calculated in a direct way. In Fig. 5 we display the product $xf(x)$ for both models again using current and constituent quark masses in the LFWF. We use the same parameters as in Table I.

In principle, contributions from higher Fock states should be added because they are not necessarily small. In fact, in the pion case that we are discussing here, the valence state component is around 25% as can be seen in Table I or, for example, in Refs. [25,26].

IV. EXAMPLE II: DECAY CONSTANTS

Now we are in the position to calculate leptonic couplings of pseudoscalar (f_P) and vector (f_V) mesons which are given in our approach by

$$f_P = f_V = 2\sqrt{6}\int_0^1 dx \int \frac{d^2\mathbf{k}_\perp}{16\pi^3}\psi_{q\bar{q}}(x, \mathbf{k}_\perp). \qquad (36)$$

We use experimental values for the decay constants and the probability condition

$$P_{q\bar{q}} = \int_0^1 dx \int \frac{d^2\mathbf{k}_\perp}{16\pi^3}|\psi_{q\bar{q}}(x, \mathbf{k}_\perp)|^2 \leq 1, \qquad (37)$$

where the equality holds for the case when the valence part dominates. This procedure allows to fix the parameters $\kappa_{1,2}$ and the normalization constants $A_{1,2}$.

Holographic models usually give a relation between $\kappa_{1,2}$ and the Regge slope fixed by spectroscopic data. Thus the only free parameter $A_{1,2}$ can be fixed by the normalization condition. As an example we consider the decay constant for kaons and J/ψ assuming the valence contribution to be dominant, i.e. we use (37) with $P_{q\bar{q}} = 1$. The quark masses used are

$$m_u = m_d = 330 \text{ MeV}, \qquad m_s = 500 \text{ MeV},$$
$$m_c = 1500 \text{ MeV}.$$

As already mentioned, the parameters $\kappa_{1,2}$ can be fixed by using Regge slope data [31,32]: for kaon we take $\kappa_1 = \kappa_2 = 524$ MeV [31], while for J/ψ we use $\kappa_1 = \kappa_2 = 894$ MeV.

Now we can calculate the decay constants of K and J/ψ mesons. In Model 1 we obtain: $f_K = 156.01$ MeV and $f_{J/\psi} = 226.68$ MeV. Our predictions in Model 2 are: $f_K = 156.35$ MeV and $f_{J/\psi} = 224.97$ MeV. Our results for the π and K meson decay constants in both models are close to the experimental values of 155.5 and 277.6 MeV, respectively.

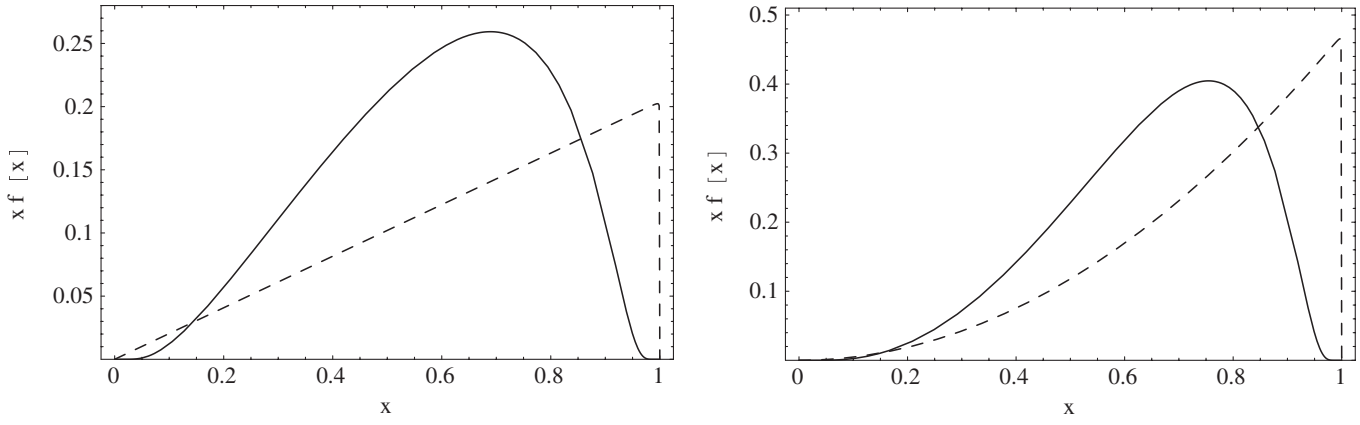

FIG. 5. Valence parton distribution $xf(x)$ according to the LFWF considered in this work. The right graph corresponds to model 1 and the left graph is for model 2. In both cases the dashed line corresponds to the case with current masses, while the solid line correspond to the constituent mass case. The parameters involved are the same as displayed in Table I.

Further applications of the approach considered here to the mass spectrum and decay constants of light and heavy hadrons will be considered in Ref. [33].

V. CONCLUSIONS

We have considered two kinds of wave functions for mesons in the light-front formalism, obtained by the AdS/CFT correspondence within two soft-wall holographic models. By identifying in the momentum space wave function the kinetic energy in the massless case we could introduce the quark mass dependence as suggested by Brodsky and de Teramond [24]. These wave functions have different x dependence, which is less pronounced when the quark masses are increased, as can be seen in Figs. 1–3. This different x dependence is due to the fact that the mode dual to the electromagnetic current $J(Q^2, z)$ is different in both models, which according to (5) translates into a different $g(x)$ and therefore a different x dependence in the corresponding LFWFs. If we restrict ourselves to pions, there is an asymmetry in (26) which does not appear in (17), because in model 1 we have $g(x) = 1$ and in model 2 we have $g(x) = 2x$.

When other mesons are considered, the parameter $\kappa_{1,2}$ used in the holographic models can be fixed by spectroscopic data, since this parameter is related to the corresponding Regge trajectory. Taking quark masses as initial input only one parameter remains (the normalization constant $A_{1,2}$), which can be fixed by the normalization condition.

Properties such as the pion decay constant or electromagnetic form factors have been studied in holographical models only in the AdS side [34]. In this work we considered expressions obtained in the CFT side, which are related to a mesonic wave function, obtained using Gauge/Gravity ideas. Because of the importance of the hadronic wave function in QCD the versions considered in this work represent a clear example of the usefulness of the AdS/CFT ideas in QCD applications. These wave functions can be used as initial ansatz in variational treatments or as a first step in order to diagonalize the light-front QCD Hamiltonian.

Another aspect that was not considered here is related to the fact that the AdS modes dual to mesons have a dependence on n and L [13,25], the radial and angular quantum numbers, respectively. Thus in principle it should be possible to obtain LFWFs for radial and angular excitations also. The Gauge/Gravity dualities offer an interesting opportunity to consider different meson excitations and in future work we plan to see whether these models reproduce the corresponding data.

ACKNOWLEDGMENTS

The A. V. work was partially supported by DGIP from Universidad Técnica Federico Santa María. A. V. is grateful for the hospitality of the Institut für Theoretische Physik of Universität Tübingen, where this work started. This work was supported by the DFG under Contract No. FA67/31-1, No. FA67/31-2, and No. GRK683. This research is also part of the European Community-Research Infrastructure Integrating Activity ''Study of Strongly Interacting Matter'' (HadronPhysics2, Grant Agreement No. 227431) and of the President grant of Russia ''Scientific Schools'' No. 871.2008.2.

[1] E. E. Salpeter and H. A. Bethe, Phys. Rev. **84**, 1232 (1951).
[2] H. C. Pauli and S. J. Brodsky, Phys. Rev. D **32**, 1993 (1985); **32**, 2001 (1985).
[3] S. J. Brodsky, C. R. Ji, and M. Sawicki, Phys. Rev. D **32**, 1530 (1985).
[4] O. C. Jacob and L. S. Kisslinger, Phys. Lett. B **243**, 323 (1990).
[5] J. Polchinski and M. J. Strassler, Phys. Rev. Lett. **88**, 031601 (2002).
[6] R. A. Janik and R. B. Peschanski, Nucl. Phys. **B565**, 193 (2000).
[7] S. J. Brodsky and G. F. de Teramond, Phys. Lett. B **582**, 211 (2004).
[8] E. Levin, J. Miller, B. Z. Kopeliovich, and I. Schmidt, J. High Energy Phys. 02 (2009) 048.
[9] G. F. de Teramond and S. J. Brodsky, Phys. Rev. Lett. **94**, 201601 (2005).
[10] A. Karch, E. Katz, D. T. Son, and M. A. Stephanov, Phys. Rev. D **74**, 015005 (2006).
[11] H. Forkel, M. Beyer, and T. Frederico, J. High Energy Phys. 07 (2007) 077.
[12] A. Vega and I. Schmidt, Phys. Rev. D **78**, 017703 (2008).
[13] A. Vega and I. Schmidt, Phys. Rev. D **79**, 055003 (2009).
[14] L. Da Rold and A. Pomarol, Nucl. Phys. **B721**, 79 (2005).
[15] J. Erlich, E. Katz, D. T. Son, and M. A. Stephanov, Phys. Rev. Lett. **95**, 261602 (2005).
[16] P. Colangelo, F. De Fazio, F. Giannuzzi, F. Jugeau, and S. Nicotri, Phys. Rev. D **78**, 055009 (2008).
[17] H. Boschi-Filho, N. R. F. Braga, and C. N. Ferreira, Phys. Rev. D **73**, 106006 (2006); **74**, 089903(E) (2006).
[18] O. Andreev and V. I. Zakharov, Phys. Rev. D **74**, 025023 (2006).
[19] F. Jugeau, arXiv:0812.4903.
[20] T. Hambye, B. Hassanain, J. March-Russell, and M. Schvellinger, Phys. Rev. D **74**, 026003 (2006); **76**, 125017 (2007).
[21] S. J. Brodsky and G. F. de Teramond, Phys. Rev. Lett. **96**, 201601 (2006).

[22] S. J. Brodsky and G. F. de Teramond, Phys. Rev. D **77**, 056007 (2008).
[23] S. J. Brodsky and G. F. de Teramond, AIP Conf. Proc. **1116**, 311 (2009).
[24] See, e.g., S. J. Brodsky and G. F. de Teramond, arXiv:0802.0514.
[25] T. Huang, B. Q. Ma, and Q. X. Shen, Phys. Rev. D **49**, 1490 (1994).
[26] S. J. Brodsky, T. Huang, and G. P. Lepage, *Proceedings of the Banff Summer Institute on Particles and Fields 2, Banff, Alberta, 1981*, edited by A. Z. Capri and A. N. Kamal (Plenum, New York, 1983), p. 143; P. Lepage, S. J. Brodsky, T. Huang, and P. B. Mackenzie, *ibid.*, p. 83; T. Huang, AIP Conf. Proc. **68**, 1000 (1980).
[27] See, e.g., W. J. Metcalf *et al.*, Phys. Lett. B **91**, 275 (1980).
[28] G. P. Lepage and S. J. Brodsky, Phys. Rev. D **22**, 2157 (1980).
[29] G G. P. Lepage and S. J. Brodsky, Phys. Lett. B **87**, 359 (1979).
[30] A. V. Radyushkin, Phys. Rev. D **58**, 114008 (1998).
[31] F. Iachello, N. C. Mukhopadhyay, and L. Zhang, Phys. Rev. D **44**, 898 (1991).
[32] S. S. Gershtein, A. K. Likhoded, and A. V. Luchinsky, Phys. Rev. D **74**, 016002 (2006).
[33] T. Branz, T. Gutsche, S. Kovalenko, V. E. Lyubovitskij, I. Schmidt, and A. Vega (unpublished).
[34] See, e.g., H. R. Grigoryan and A. V. Radyushkin, Phys. Rev. D **76**, 115007 (2007); H. J. Kwee and R. F. Lebed, J. High Energy Phys. 01 (2008) 027; Phys. Rev. D **77**, 115007 (2008).